HHS Public Access

Author manuscript

J Invest Dermatol. Author manuscript; available in PMC 2023 February 01.

Published in final edited form as:

J Invest Dermatol. 2022 February ; 142(2): 314–322. doi:10.1016/j.jid.2021.06.031.

Interferon regulatory factor 6 regulates the delivery of E-cadherin to the plasma membrane

Angelo Antiguas[1], **Kris A. DeMali**[2], **Martine Dunnwald**[1]

[1]Department of Anatomy and Cell Biology, The University of Iowa, IA, 52242

[2]Department of Biochemistry and Dermatology, The University of Iowa, IA, 52242

Abstract

Interferon Regulatory Factor 6 (IRF6) is a transcription factor that is required for craniofacial development and epidermal morphogenesis. Specifically, *Irf6*-deficient mice lack the terminally differentiated epidermal layers, leading to the absence of barrier function. This phenotype also includes intraoral adhesions due to the abscence of the oral periderm, leading to the mislocalization of E-cadherin and other cell-cell adhesion proteins of the oral epithelium. However, the mechanisms by which IRF6 control the localization of cell adhesion proteins is not understood. Here, we demonstrate that, in human and murine keratinocytes, loss of IRF6 leads to breakdown of epidermal sheets following mechanical stress. This defect is due to a reduction of adhesion proteins at the plasma membrane. Dynamin inhibitors rescued the IRF6-dependent resistance of epidermal sheets to mechanical stress, but only inhibition of clathrin-mediated endocytosis rescued the localization of junctional proteins at the membrane. Our data show that E-cadherin recycling, but not its endocytosis, is affected by loss of IRF6. Overall, we demonstrate a role for IRF6 in the delivery of adhesion proteins to the cell membrane.

INTRODUCTION

Epithelia are highly organized tissues lining most organs, including the outermost surface of our body and the oral cavity. Epithelia, and particularly the epidermis of the skin, protect the organism from mechanical, chemical and microbial attacks by functioning as a biologically impermeable barrier (Madison 2003). Critical to this barrier function are intercellular adhesions between keratinocytes of the epidermis, including adherens junctions (AJ), desmosomes, and tight junctions (Morita et al. 1998; Furuse et al. 2002; Schlüter et al. 2004).

Corresponding author: Martine Dunnwald, PharmD, PhD, 1-532 BSB, Anatomy and Cell Biology Department, The University of Iowa, 51 Newton Road, Iowa City, IA 52242, Tel: 319 384 4645, martine-dunnwald@uiowa.edu.

AUTHOR CONTRIBUTIONS

Conceptualization and writing: AA, KAD, MD; Formal analysis: AA, MD; Funding acquisition: MD

CONFLICT OF INTERETS

The authors state no conflict of interest

Adherens junctions are highly evolutionary conserved inter-cellular structures, forming continuous adhesion belts along the apical-lateral interface of neighboring cells. These structures link the actin cytoskeleton of neighboring cells, thereby providing mechanical resistance, as well as the molecular machinery to sense and generate forces from one cell to another (Tunggal et al. 2005; Mertz et al. 2013; Ohashi et al. 2017; Yap et al. 2018). The molecular components of AJ include members of the armadillo protein family such as β-catenin, α-catenin and p120-catenin, and clusters of calcium-dependent cell adhesion receptor from the cadherin family, including E-cadherin (Behrens et al. 1985; Gumbiner et al. 1988; Nagafuchi and Takeichi 1988; Takeichi 1991; Adams et al. 1996).

E-cadherin is a transmembrane protein synthesized in the endoplasmic reticulum and delivered to the cell membrane through the secretory pathway (Geng et al. 2012). This molecule is highly dynamic, undergoing continuous cycles of endocytosis, sorting and recycling back to the plasma membrane. Transcriptional regulation of E-cadherin is relatively slow (Cavey and Lecuit 2009) and does not account for the fast processes necessary for cell adhesion rearrangement during morphogenesis and tissue repair. Instead, E-cadherin is constantly internalized from the plasma membrane through several endocytic mechanisms, including clathrin mediated endocytosis (Palacios et al. 2002). After internalization, E-cadherin localizes to early, then recycling endosomes (Wandinger-Ness and Zerial 2014), and is delivered back to the plasma membrane or toward multivesicular endosomes that fuse to the lysosome for later degradation (Hunter et al. 2015).

Interferon regulatory factor 6 (IRF6) belongs to the interferon regulatory factor (IRF) family of transcription factors (Taniguchi et al. 2001) and has been implicated in craniofacial, limb and epidermal development (Ingraham et al. 2006). *Irf6*-deficient embryos lack the granular and cornified layers that confer the barrier function to the skin. They also lack the oral periderm, exhibit ectopic localization of E-cadherin and other cell-cell adhesion proteins, which ultimately lead to intraoral tissue adhesion and a complete fusion of the oral cavity. Disruption of these adhesion proteins in the absence of IRF6 ultimately leads to postnatal lethality (Ingraham et al. 2006). However, how IRF6 regulates the localization of intercellular adhesion proteins is poorly understood.

In the present study, using a combination of primary murine keratinocytes and human keratinocyte cell lines with decreased levels of IRF6, we show that IRF6 is required for proper delivery of E-cadherin to the plasma membrane.

RESULTS

Human IRF6 knockdown keratinocytes fail to differentiate in vitro

In order to generate human cell lines deficient for IRF6, we designed shRNAs specifically targeting *IRF6*-mRNA in a human foreskin keratinocyte (HFK) cell line (Darbro et al. 2005). Following calcium-induced *in vitro* differentiation, wild-type keratinocytes upregulated IRF6, whereas two out of three shRNA lines showed minimal levels of IRF6 (Figure S1a, b and data not shown). Based on these results, we further characterized the 495 line (further referred to as shIRF6). Phase contrast analysis demonstrated the presence of stratified areas with loss of keratin (K) 14 and upregulation of K10 in wild-

type keratinocytes (Figure S1c, d). However, the shIRF6 keratinocytes were unable to differentiate, as demonstrated by the maintainance of K14, and decrease in K10-positive keratinocytes (Figure S1c, d). Total RhoA GTPase levels were unchanged in IRF6 knockdown cells, however GTP-bound RhoA (the active form) levels were increased in shIRF6 keratinocytes (Figure S1e). Combined, these results demonstrate that human shIRF6 keratinocytes exhibit characteristics similar to what we previously described for *Irf6*-deficient murine keratinocytes (Biggs et al. 2012).

IRF6 is required for keratinocyte monolayer resistance to mechanical stress

Based on the observation that *Irf6*-deficient murine epidermis showed altered localization of cell-cell adhesion components (Richardson et al. 2014), and their well-established roles in the mechanical properties of tissues, we hypothesized that keratinocyte monolayers require IRF6 to resist to mechanical stress. To test our hypothesis, Dispase-treated HFK and shIRF6 monolayers were exposed to mechanical disruption (Figure 1a). The resulting number of fragments in suspension was significantly higher in shIRF6 keratinocytes compared to wild-type (Figure 1a), demonstrating that IRF6 is required for the resistance of the keratinocyte monolayer to mechanical stress.

IRF6 is required for proper subcellular localization of AJ proteins

We sought to gain mechanistic insight into the cause of IRF6-dependent resistance of keratinocyte monolayers to mechanical stress. We first examined whether IRF6 was required for the assembly of AJ. The initial step of junction assembly is cadherin engagement, which is based on interactions between two E-cadherin extracellular domains of adjacent cells. We measured the adhesions of HFK and shIRF6 keratinocytes to culture dishes coated with extracellular domain of E-cadherin. shIRF6 keratinocytes were reduced in their adhesion to this substrate compared with wild-type cells (Figure 1b), supporting the functional importance of IRF6 for E-cadherin adhesion. Yet, they do not distinguish between a potential impairement of E-cadherin adhesion function itself and E-cadherin localization.

We then assessed the subcellular localization of E-cadherin following calcium-induced formation of cell-cell adhesions. By immunofluorescence, we observed that wild-type keratinocytes formed continuous E-cadherin adhesion zippers at the junction between two adjacent cells, whereas *Irf6*-deficient cells and shIRF6 keratinocytes showed a discontinuous focal pattern of E-cadherin (Figure 1c, and data not shown). Furthermore, the intensity of the fluorescent signal at the cell membrane was reduced in shIRF6 keratinocytes (Figure 1c). In these same cells, however, total cellular levels of E-cadherin were unchanged when compared with wild-type keratinocytes (Figure 1d and S2a). A similar defect was observed with beta-catenin and vinculin (Figure 1e and Figure S2b–e). We conclude that IRF6 is required for proper localization, but not overall protein levels, of AJ components to the cell membrane, affecting cell adhesion.

IRF6 is required for proper subcellular localization of tight junctions and desmosomal proteins

There is extensive evidence suggesting adherens junctions participate in the assembly and proper functioning of tight junctions (Rajasekaran et al. 1996; Müller et al. 2005; Ooshio

et al. 2010; Maiers et al. 2013; Rübsam et al. 2017) and desmosomes (Shafraz et al. 2017). We hypothesized that in the absence of IRF6, defective AJ would lead to disruption of the signaling processes orchestrating proper formation of tight junctions and desmosomes. In support of our hypothesis, we observed a discontinuous pattern of ZO1, Occludin and Desmoplakin at the cell membrane of *Irf6*-deficient keratinocytes following calcium-induced adhesion, compared to wild-type cells (Figure 2), while Occludin total cellular levels were unchanged (Figure S2f). Overall, our data support a model in which decreased IRF6 leads to the disruption not only of the formation of AJ, but also of other cell adhesions that may require AJ-dependent signals for their own assembly.

Inhibition of dynamin-dependent endocytosis rescues E-cadherin localization to the plasma membrane

The availability and levels of E-cadherin at the plasma membrane are determined by the balance between the delivery and recycling of E-cadherin to the membrane, and the rate of E-cadherin endocytosis (Brüser and Bogdan 2017). To investigate whether the IRF6-dependent reduction of E-cadherin levels at the membrane was due to a defect in endocytosis, we treated HFK and shIRF6 keratinocytes with Dyngo-4a, a potent inhibitor of dynamin-mediated endocytosis. As shown in Figure 3a, Dyngo-4a-treated shIRF6 keratinocytes showed increase levels of E-cadherin at the membrane to the levels of the wild-type cells. Dyngo-4a treatment also restored the linear pattern of ZO-1 similar to wild-type, but not its intensity level after 24 h of treatment (Figure S3). However, Dyngo-4a did not improve the discontinuous pattern and intensity levels at the membrane of Occludin and Desmoplakin in shIRF6 (Figure S3). Concomitantly, the resistance to mechanical stress of shIRF6 keratinocyte monolayers treated with Dyngo-4a was restored to that of wild-type cells (Figure 3b). These results could be due to 1) Inhibition of dynamin, maintaining delivered E-cadherin at the cell membrane, leading to an accumulation of E-cadherin to an equivalent level between wild-type and shIRF6 keratinocytes, or 2) an increase in E-cadherin endocytosis.

Rate of endocytosis is not affected by IRF6

To distinguish between our two hypothesis, we first investigated the localization of p120-catenin in the context of IRF6. P120-catenin is a master regulator of E-cadherin endocytosis that binds to E-cadherin cytoplasmic tail and prevents its interactions with the endocytic membrane trafficking machinery (Davis et al. 2003; Nanes et al. 2016). Our results show that in keratinocytes with reduced levels of IRF6, p120-catenin pattern of expression was similar to that of E-cadherin in wild-type (continuous) and shIRF6 (focal and discontinuous) keratinocytes. The intensity of the immunofluorescent signal for p120-catenin at the cell membrane was also decreased compared to the wild-type cells, yet overall protein levels were unchanged between groups (Figure 3c and Figure S2g).

To formaly determine if endocytosis contributes to our observations, we performed biotinylation of cell membrane proteins. As shown in Figure 3d, total lysates (Input) showed equal levels of E-cadherin in both cell lines maintained at 4°C (T0) and following 1 h at 37°C (T1), consistent with our results shown in Figure 1d. However, following streptavidin pull down (Pull down, Figure 3d), steady-state E-cadherin levels at the membrane (T0) were

reduced in shIRF6 keratinocytes compared with wild-type cells, consistent with data shown in Figure 1c. Surprisingly, the rate of endocytosis, calculated as the ratio of E-cadherin levels between T0 and T1, was similar between HFK and shIRF6 keratinocytes (Figure 3d). Collectively, these results confirm that E-cadherin levels at the plasma membrane are reduced in keratinocytes with reduced IRF6 levels, and that increased rate of E-cadherin endocytosis is not contributing to this defect.

Decreased recycling of E-cadherin to the plasma membrane contributes to the IRF6-dependent cell adhesion defect

If IRF6 levels do not affect the rate of endocytosis, we hypothesized that IRF6 promotes the delivery of E-cadherin to the cell membrane. To test our hypothesis, we transfected HFK and shIRF6 keratinocytes with E-cadherin-GFP expressing plasmid and performed fluorescence recovery after photobleaching of membrane bound E-cadherin-GFP. We found that the fluorescence recovery rate and the recovered fraction were both significantly decreased in human and murine keratinocytes with reduced levels of IRF6 compared with wild-type cells (Figure 4a and data not shown), suggesting that IRF6 is required for the delivery of E-cadherin to the membrane. Consequently, we asked whether E-cadherin would accumulate away from the plasma membrane. Following immunofluorescent staining, we quantified the number of E-cadherin-positive puncta (Figure 4b, c) and found no differences in the number of puncta between HFK and shIRF6 keratinocytes. An extended analysis of the area and the intensity of the E-cadherin positive puncta, however, showed that both were significantly increased in shIRF6 compared with wild-type keratinocytes (Figure 4c), suggesting an accumulation of E-cadherin away from the plasma membrane.

To investigate a function for IRF6 in E-cadherin recycling, we performed an internalization assay (Figure 4d). Although the membrane levels of E-cadherin were reduced in shIRF6 keratinocytes (Figure 4e), the internalized E-cadherin did not recycle back to the plasma membrane (Figure 4f), and fewer cells had E-cadherin at the membrane (Figure 4f), complementing results of Figure 3 showing unperturbed endocytosis in shIRF6 cells. Thus, loss of IRF6 leads to vesicular accumulation of E-cadherin, and to a defective recycling to the plasma membrane, ultimately resulting in a reduction of E-cadherin levels at the membrane.

DISCUSSION

Much attention has been devoted towards identifying roles for IRF6 in epithelial differentiation. A few studies have also reported a role for IRF6 in tissue adhesions, with the implication that this transcription factor could regulate cell-cell adhesions (Richardson et al. 2014). However, very little attention has been given to which particular cellular processes are regulated by IRF6 to control cell-cell adhesion. Our study demonstrates, in human and murine keratinocytes, that IRF6 is needed for keratinocyte resistance to mechanical stress. This defect is due to a reduction of adhesion proteins at the plasma membrane. Particularly, we show that IRF6 is required for the recycling of E-cadherin at the plasma membrane, identifying a previously unreported function for this transcription factor in regulating adhesion protein dynamics.

Cell-cell adhesions are essential structures that maintain cohesiveness between epithelial cells to form tissues. All of the cell-cell adhesion complexes were affected by the loss of IRF6 in keratinocytes, with significantly decreased protein levels at the plasma membrane (Figures 1, 2, S2). We speculate that it is the effect of IRF6 on E-cadherin-mediated adhesion that led to alterations in other junctional complexes, based on previous evidence that adherens junctions are the initial cell-cell contacts formed between two neighboring cells (Rajasekaran et al. 1996; Müller et al. 2005; Ooshio et al. 2010; Maiers et al. 2013; Rübsam et al. 2017). Consequently, the increased localization of E-cadherin at the membrane following dynamin inhibitor treatment partially rescued the localization of other junctional complexes within the time frame of the experiment. The levels of E-cadherin at the plasma membrane thus would influence the recruitment of tight junction and desmosomal components, although we can not rule out a direct effect of IRF6 on these components.

The reduction of E-cadherin at the membrane that occurs with the loss of IRF6 could be due to several mechanisms, including 1) a decrease in overall protein level, 2) an increase in endocytosis, or 3) a decrease in trafficking/recycling (delivery) to the membrane. We tested all three possibilities. Our data conclude that IRF6 is necessary for the delivery of endocytosed E-cadherin to the plasma membrane. Previous studies have shown that transcript levels of E-cadherin and other AJ proteins in the epidermis and keratinocytes in cultures were not significantly changed between IRF6-deficient and control samples (Ingraham et al. 2006; Botti et al. 2011). Our data obtained with protein extracts complement these earlier observations, suggesting that IRF6, although structurally characterized as a transcription factor, is not regulating these molecules directly at the transcriptional level. Our studies do not distinguish whether IRF6 promotes the membrane localization of junctional proteins via a transcriptional role facilitating intracellular trafficking or via a non-transcriptional protein-protein interaction. A non-traditional cytoplasmic function for IRF6 has been speculated in the context of palatogenesis (Parada-Sanchez et al. 2017), and we and others have previously published studies in which IRF6 is mainly detected in the cytoplasm (Bailey et al. 2005; Little et al. 2009; Biggs et al. 2012). Additionally, studies of patient-derived mutations demonstrated that the IRF6 protein binding domain contributes to both its transcriptional and non-transcriptional function (Little et al. 2009). Such dual nuclear transcriptional activity and cytoplasmic protein regulation have been described for β-catenin (Takeichi 1991; Tao et al. 1996) and Grainyhead-like 3 (GRHL3) (Kimura-Yoshida et al. 2018). GRHL3 is particularly interesting as it belongs to the IRF6 gene-regulatory network, and mutations in *GRHL3*, like in *IRF6*, lead to Van der Woude syndrome (Peyrard-Janvid et al. 2014). Further investigations would determine if indeed IRF6 has a cytoplasmic function similar to GRHL3.

Although the use of Dyngo-4a rescued both E-cadherin intensity at the membrane and resistance to mechanical stress, we believe these results are the consequence of an accumulation of E-cadherin at the membrane in the presence of the dynamin inhibitor. p120-catenin, which is required to stabilize E-cadherin at the membrane and prevent it from being endocytosed (Davis et al. 2003), was also at the membrane, providing further evidence that endocytosis is not affected by IRF6 levels. We did observe, however, lower levels of p120-catenin at the plasma membrane of *Irf6*-deficient keratinocytes, which could

be the consequence of the diminished levels of E-cadherin anchoring p120-catenin at sites of cell-cell junctions.

Collectively, our results desmontrated that IRF6 is required for E-cadherin delivery to the plasma membrane. Keratinocytes with reduced IRF6 displayed impaired E-cadherin dynamics by both FRAP and *in vitro* internalization assays. Interestingly, cytoplasmic IRF6 was recently shown to bind Nucleoside Diphosphate Kinase B (NME1), a highly conserved 18 kDa Guanine-nucleotide Exchange Factors regulating the activity of small GTPases, known to regulate E-cadherin dynamics (Palacios et al. 2002), and in which mutations were reported in two patients with cleft lip and palate (Parada-Sanchez et al. 2017). We speculate that reduced IRF6 protein levels would affect the function of NME1. Molecular manipulations of NME1 in the context of IRF6-dependent E-cadherin turnover would be required to determine whether this interaction is responsible for our observations.

In conclusion, our work identified a previously unreported function for IRF6 in modulating E-cadherin delivery to the plasma membrane. E-cadherin dynamics have been described as central to cancer biology (Zhang et al. 2006). IRF6 has been previously characterized as a tumor suppressor (Botti et al. 2011) and identified as a regulator of epithelial migration (Biggs et al. 2014). Therefore, our studies provide a mechanistic insight on how IRF6 could contribute to cancer and wound healing.

MATERIALS and METHODS

Detailed material and methods are provided in the Supplementary Materials associated with this paper.

shIRF6 cell lines generation

pSUPER-shIRF6 was used to silence endogenous IRF6 in human foreskin keratinocyte cell lines (HFK) (Darbro et al. 2005).

Keratinocyte culture

Mouse husbandry was consistent with the Animal Care and Use Review Form at the University of Iowa. Murine primary keratinocytes were obtained from e17.5 embryonic skin (Biggs et al. 2012). HFK were maintained in keratinocyte serum-free medium (KSFM, Gibco, Waltham, MA). To induce the formation of Ca^{2+}-dependent cell junctions, cells were switched from media with 0.15 mM $CaCl_2$ (referred thereafter to low [Ca^{2+}]), to medium with an additional 1.5 mM $CaCl_2$ (referred thereafter to high [Ca^{2+}]). Y27632 (Sigma, St Louis, MO) and Dyngo-4a (Abcam, Cambrifge, MA) were used at 10 mM and 10 μM, respectively.

Dispase assay

Confluent human keratinocytes were cultured in 1.5 mM for 24 h then incubated in 2.5 U/ml Dispase II (Roche Applied Science, Penzberg, Germany) for 30 min at 37°C. The keratinocyte monolayer was mechanically disrupted following 10 repeated pipetting with a 5 ml Stripette.

E-cadherin FC adhesion assay

Quantification of the adhesion of cells to E-cadherin FC coated plates was performed as previously described (Bays et al. 2017). Keratinocytes were seeded onto E-cadherin FC coated plates and allowed to attach for 1 h in high [Ca^{2+}] medium. Images from four equally sized quadrants were taken from each well and attached cells were counted using ImageJ.

Biotinylation assay

Biotin solution was added to high [Ca^{2+}] treated confluent keratinocytes. Biotinylation assay was performed as previously described (Graeve et al. 1989).

Fluorescent recovery after photobleaching (FRAP)

E-cadherin-GFP (423) was a gift from Alpha Yap (Addgene plasmid # 677937, Watertown, MA, (Truffi et al. 2014)) and transfected in human and murine keratinocytes. Bleaching of fluorescence was performed at room temperature on the cell membrane of two adjacent cells expressing E-cadherin GFP using the 488 nm laser of a Zeiss LSM 700 confocal microscope and images taken every 60 sec until achieving a plateau. Fluorescent recovery was quantified as a percent of initial E-cadherin-GFP membrane intensity.

Internalization assay

An internalization assay was performed as previously described (Xiao et al. 2003; Chiasson et al. 2009; Nanes et al. 2016).

Data Availability Statement

No datasets were generated during the current study.

Supplementary Material

Refer to Web version on PubMed Central for supplementary material.

ACKNOWLEDGEMENTS

The authors would like to thank Lindsey Rhea for critical reading of the manuscript. This work was supported by grants from the National Institute of Health (R01AR067739 to M.D; R01AR067739 minority supplement to A.A; R35GM136291 to K.A.D).

REFERENCES

Adams CL, Nelson WJ, Smith SJ. Quantitative analysis of cadherin-catenin-actin reorganization during development of cell-cell adhesion. J Cell Biol 1996 Dec 15;135(6):1899–911. [PubMed: 8991100]

Bailey CM, Khalkhali-Ellis Z, Kondo S, Margaryan NV, Seftor REB, Wheaton WW, et al. Mammary Serine Protease Inhibitor (Maspin) Binds Directly to Interferon Regulatory Factor 6. J Biol Chem 2005 Oct 7;280(40):34210–7. [PubMed: 16049006]

Bays JL, Campbell HK, Heidema C, Sebbagh M, DeMali KA. Linking E-cadherin mechanotransduction to cell metabolism through force-mediated activation of AMPK. Nat Cell Biol 2017 Jun;19(6):724–31. [PubMed: 28553939]

Behrens J, Birchmeier W, Goodman SL, Imhof BA. Dissociation of Madin-Darby Canine Kidney Epithelial Cells by the Monoclonal Antibody Anti-Arc-l: Mechanistic Aspects and Identification of the Antigen as a Component Related to Uvomorulin. J CELL Biol 1985;101:9.

Biggs LC, Naridze RL, DeMali KA, Lusche DF, Kuhl S, Soll DR, et al. Interferon regulatory factor 6 regulates keratinocyte migration. J Cell Sci 2014 Jul 1;127(13):2840–8. [PubMed: 24777480]

Biggs LC, Rhea L, Schutte BC, Dunnwald M. Interferon Regulatory Factor 6 Is Necessary, but Not Sufficient, for Keratinocyte Differentiation. J Invest Dermatol 2012 Jan;132(1):50–8. [PubMed: 21918538]

Botti E, Spallone G, Moretti F, Marinari B, Pinetti V, Galanti S, et al. Developmental factor IRF6 exhibits tumor suppressor activity in squamous cell carcinomas. Proc Natl Acad Sci 2011 Aug 16;108(33):13710–5. [PubMed: 21807998]

Brüser L, Bogdan S. Adherens Junctions on the Move—Membrane Trafficking of E-Cadherin. Cold Spring Harb Perspect Biol 2017 Mar 1;9(3):a029140. [PubMed: 28096264]

Cavey M, Lecuit T. Molecular Bases of Cell-Cell Junctions Stability and Dynamics. Cold Spring Harb Perspect Biol 2009 Nov 1;1(5):a002998–a002998. [PubMed: 20066121]

Chiasson CM, Wittich KB, Vincent PA, Faundez V, Kowalczyk AP. p120-Catenin Inhibits VE-Cadherin Internalization through a Rho-independent Mechanism. Mol Biol Cell. 2009 Feb 11;20(7):1970–80. [PubMed: 19211843]

Darbro BW, Schneider GB, Klingelhutz AJ. Co-Regulation of p16INK4a and Migratory Genes in Culture Conditions that Lead to Premature Senescence in Human Keratinocytes. J Invest Dermatol 2005 Sep;125(3):499–509. [PubMed: 16117791]

Davis MA, Ireton RC, Reynolds AB. A core function for p120-catenin in cadherin turnover. J Cell Biol 2003 Nov 10;163(3):525–34. [PubMed: 14610055]

Furuse M, Hata M, Furuse K, Yoshida Y, Haratake A, Sugitani Y, et al. Claudin-based tight junctions are crucial for the mammalian epidermal barrier. J Cell Biol 2002 Mar 18;156(6):1099–111. [PubMed: 11889141]

Geng F, Zhu W, Anderson RA, Leber B, Andrews DW. Multiple post-translational modifications regulate E-cadherin transport during apoptosis. J Cell Sci 2012 Jun 1;125(11):2615–25. [PubMed: 22375065]

Graeve L, Drickamer K, Rodriguez-Boulan E. Polarized endocytosis by Madin-Darby canine kidney cells transfected with functional chicken liver glycoprotein receptor. J Cell Biol 1989 Dec;109(6 Pt 1):2809–16. [PubMed: 2687287]

Gumbiner B, Stevenson B, Grimaldi A. The role of the cell adhesion molecule uvomorulin in the formation and maintenance of the epithelial junctional complex. J Cell Biol 1988 Oct 1;107(4):1575–87. [PubMed: 3049625]

Hunter MV, Lee DM, Harris TJC, Fernandez-Gonzalez R. Polarized E-cadherin endocytosis directs actomyosin remodeling during embryonic wound repair. J Cell Biol 2015 Aug 31;210(5):801–16. [PubMed: 26304727]

Ingraham CR, Kinoshita A, Kondo S, Yang B, Sajan S, Trout KJ, et al. Abnormal skin, limb and craniofacial morphogenesis in mice deficient for interferon regulatory factor 6 (Irf6). Nat Genet 2006 Nov;38(11):1335–40. [PubMed: 17041601]

Kapetanovich L, Baughman C, Lee TH. Nm23H2 Facilitates Coat Protein Complex II Assembly and Endoplasmic Reticulum Export in Mammalian Cells. Mol Biol Cell. 2005 Feb;16(2):835–48. [PubMed: 15591128]

Kimura-Yoshida C, Mochida K, Nakaya M, Mizutani T, Matsuo I. Cytoplasmic localization of GRHL3 upon epidermal differentiation triggers cell shape change for epithelial morphogenesis. Nat Commun 2018 Oct 3;9(1):4059. [PubMed: 30283008]

Little HJ, Rorick NK, Su L-I, Baldock C, Malhotra S, Jowitt T, et al. Missense mutations that cause Van der Woude syndrome and popliteal pterygium syndrome affect the DNA-binding and transcriptional activation functions of IRF6. Hum Mol Genet 2009 Feb 1;18(3):535–45. [PubMed: 19036739]

Madison KC. Barrier function of the skin: “la raison d’être” of the epidermis. J Invest Dermatol 2003 Aug;121(2):231–41. [PubMed: 12880413]

Maiers JL, Peng X, Fanning AS, DeMali KA. ZO-1 recruitment to α-catenin – a novel mechanism for coupling the assembly of tight junctions to adherens junctions. J Cell Sci 2013 Sep 1;126(17):3904–15. [PubMed: 23813953]

Mertz AF, Che Y, Banerjee S, Goldstein JM, Rosowski KA, Revilla SF, et al. Cadherin-based intercellular adhesions organize epithelial cell–matrix traction forces. Proc Natl Acad Sci 2013 Jan 15;110(3):842–7. [PubMed: 23277553]

Morita K, Itoh M, Saitou M, Ando-Akatsuka Y, Furuse M, Yoneda K, et al. Subcellular Distribution of Tight Junction-Associated Proteins (Occludin, ZO-1, ZO-2) in Rodent Skin. J Invest Dermatol 1998 Jun 1;110(6):862–6. [PubMed: 9620290]

Müller SL, Portwich M, Schmidt A, Utepbergenov DI, Huber O, Blasig IE, et al. The Tight Junction Protein Occludin and the Adherens Junction Protein α-Catenin Share a Common Interaction Mechanism with ZO-1. J Biol Chem 2005 Feb 4;280(5):3747–56. [PubMed: 15548514]

Nagafuchi A, Takeichi M. Cell binding function of E-cadherin is regulated by the cytoplasmic domain. EMBO J 1988 Dec 1;7(12):3679–84. [PubMed: 3061804]

Nanes BA, Grimsley-Myers CM, Cadwell CM, Robinson BS, Lowery AM, Vincent PA, et al. p120-catenin regulates VE-cadherin endocytosis and degradation induced by the Kaposi sarcoma–associated ubiquitin ligase K5. Mol Biol Cell. 2016 Oct 26;28(1):30–40. [PubMed: 27798235]

Ohashi K, Fujiwara S, Mizuno K. Roles of the cytoskeleton, cell adhesion and rho signalling in mechanosensing and mechanotransduction. J Biochem (Tokyo). 2017 Jan 12;mvw082.

Ooshio T, Kobayashi R, Ikeda W, Miyata M, Fukumoto Y, Matsuzawa N, et al. Involvement of the Interaction of Afadin with ZO-1 in the Formation of Tight Junctions in Madin-Darby Canine Kidney Cells. J Biol Chem 2010 Feb 12;285(7):5003–12. [PubMed: 20008323]

Palacios F, Schweitzer JK, Boshans RL, D'Souza-Schorey C. ARF6-GTP recruits Nm23-H1 to facilitate dynamin-mediated endocytosis during adherens junctions disassembly. Nat Cell Biol 2002 Dec;4(12):929–36. [PubMed: 12447393]

Parada-Sanchez MT, Chu EY, Cox LL, Undurty SS, Standley JM, Murray JC, et al. Disrupted IRF6-NME1/2 Complexes as a Cause of Cleft Lip/Palate. J Dent Res 2017 Oct;96(11):1330–8. [PubMed: 28767310]

Peyrard-Janvid M, Leslie EJ, Kousa YA, Smith TL, Dunnwald M, Magnusson M, et al. Dominant Mutations in GRHL3 Cause Van der Woude Syndrome and Disrupt Oral Periderm Development. Am J Hum Genet 2014 Jan 2;94(1):23–32. [PubMed: 24360809]

Rajasekaran AK, Hojo M, Huima T, Rodriguez-Boulan E. Catenins and zonula occludens-1 form a complex during early stages in the assembly of tight junctions. J Cell Biol 1996 Feb;132(3):451–63. [PubMed: 8636221]

Richardson RJ, Hammond NL, Coulombe PA, Saloranta C, Nousiainen HO, Salonen R, et al. Periderm prevents pathological epithelial adhesions during embryogenesis. J Clin Invest 2014 Sep 2;124(9):3891–900. [PubMed: 25133425]

Rübsam M, Mertz AF, Kubo A, Marg S, Jüngst C, Goranci-Buzhala G, et al. E-cadherin integrates mechanotransduction and EGFR signaling to control junctional tissue polarization and tight junction positioning. Nat Commun 2017 Nov 1;8(1):1250. [PubMed: 29093447]

Schlüter H, Wepf R, Moll I, Franke WW. Sealing the live part of the skin: the integrated meshwork of desmosomes, tight junctions and curvilinear ridge structures in the cells of the uppermost granular layer of the human epidermis. Eur J Cell Biol 2004 Dec;83(11–12):655–65. [PubMed: 15679110]

Shafraz OM, Stahley SN, Sankar K, Jernigan RL, Kowalczyk AP, Sivasankar S. E-Cadherin Functions as a Desmoglein Transporter that Facilitates Assembly of Nascent Desmosomes. Biophys J 2017 Feb 3;112(3):166a–7a.

Takeichi M. Cadherin cell adhesion receptors as a morphogenetic regulator. Science. 1991 Mar 22;251(5000):1451–5. [PubMed: 2006419]

Taniguchi T, Ogasawara K, Takaoka A, Tanaka N. IRF Family of Transcription Factors as Regulators of Host Defense. Annu Rev Immunol 2001;19(1):623–55. [PubMed: 11244049]

Tao YS, Edwards RA, Tubb B, Wang S, Bryan J, McCrea PD. beta-Catenin associates with the actin-bundling protein fascin in a noncadherin complex. J Cell Biol 1996 Sep 1;134(5):1271–81. [PubMed: 8794867]

Truffi M, Dubreuil V, Liang X, Vacaresse N, Nigon F, Han SP, et al. RPTPα controls epithelial adherens junctions, linking E-cadherin engagement to c-Src-mediated phosphorylation of cortactin. J Cell Sci 2014 Jun 1;127(Pt 11):2420–32. [PubMed: 24652832]

Tunggal JA, Helfrich I, Schmitz A, Schwarz H, Günzel D, Fromm M, et al. E-cadherin is essential for in vivo epidermal barrier function by regulating tight junctions. EMBO J. 2005 Mar 23;24(6):1146–56. [PubMed: 15775979]

Wandinger-Ness A, Zerial M. Rab Proteins and the Compartmentalization of the Endosomal System. Cold Spring Harb Perspect Biol 2014 Nov 1;6(11):a022616. [PubMed: 25341920]

Xiao K, Allison DF, Buckley KM, Kottke MD, Vincent PA, Faundez V, et al. Cellular levels of p120 catenin function as a set point for cadherin expression levels in microvascular endothelial cells. J Cell Biol 2003 Nov 10;163(3):535–45. [PubMed: 14610056]

Yamada S, Nelson WJ. Localized zones of Rho and Rac activities drive initiation and expansion of epithelial cell–cell adhesion. J Cell Biol 2007 Jul 23;178(3):517–27. [PubMed: 17646397]

Yap AS, Duszyc K, Viasnoff V. Mechanosensing and Mechanotransduction at Cell–Cell Junctions. Cold Spring Harb Perspect Biol 2018 Aug 1;10(8):a028761. [PubMed: 28778874]

Zhang W, Alt-Holland A, Margulis A, Shamis Y, Fusenig NE, Rodeck U, et al. E-cadherin loss promotes the initiation of squamous cell carcinoma invasion through modulation of integrin-mediated adhesion. J Cell Sci 2006 Jan 15;119(Pt 2):283–91. [PubMed: 16390868]

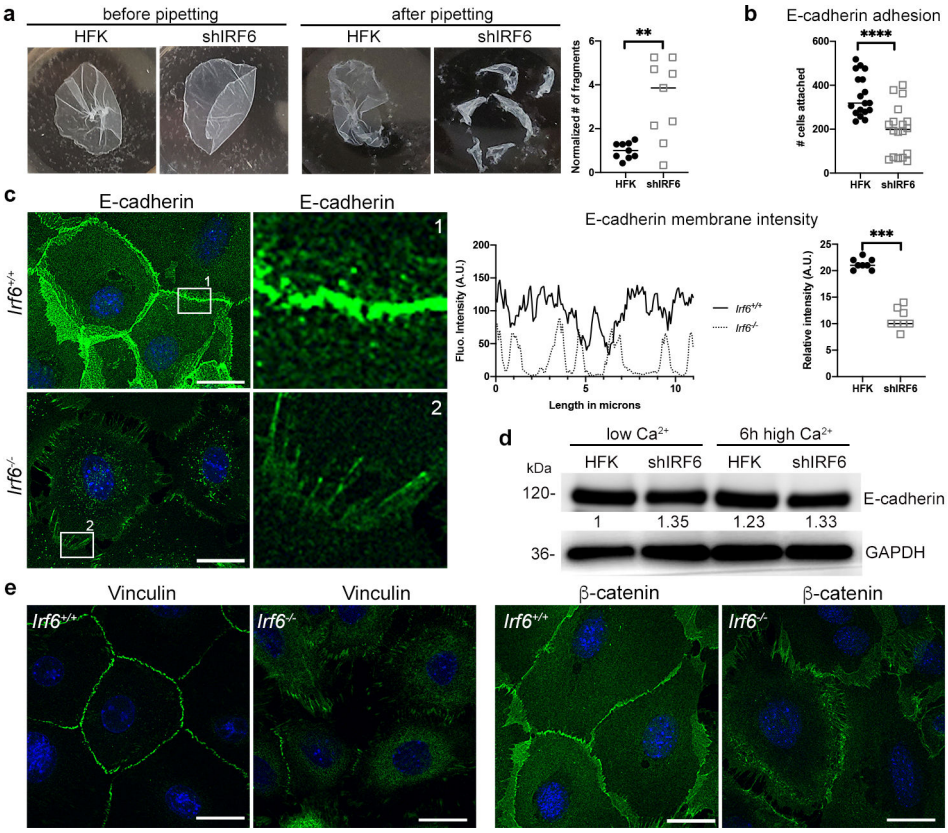

Figure 1: IRF6 is required for adherens junction assembly.

(a) Macroscopic images showing HFK and shIRF6 confluent monolayer following Dispase II treatment before and after mechanical disruption. Quantification of number of fragments per well normalized to HFK is presented on the right. **(b)** Cell attachment to extracellular domain of E-cadherin. **(c)** Immunofluorescent staining for E-cadherin (green) in *Irf6*$^{+/+}$ and *Irf6*$^{-/-}$ murine keratinocytes 6 h following high [Ca^{2+}] treatment. Nuclear DNA is labeled with DAPI (blue). Areas in white boxes 1 and 2 are presented enlarged on the right. E-cadherin pattern of intensity at the membrane is shown for these two cells. Quantification of E-cadherin intensity at the membrane is shown on the right most graph. **(d)** Western blot for E-cadherin and GAPDH (loading control) of total cellular extracts. Quantification of E-cadherin intensity is indicated by the numbers between the two panels. **(e)** Immunofluorescent staining for Vinculin (green) and β-catenin (right) of *Irf6*$^{+/+}$ and *Irf6*$^{-/-}$ murine keratinocytes 6 h following high [Ca^{2+}] treatment. Nuclear DNA is labeled with DAPI (blue). ** $P < .01$, *** $P < .001$, and **** $P < .0001$ following Kruskal-Wallis test with Dunn's multiple comparison post-hoc test. Scale bars = 10 μm

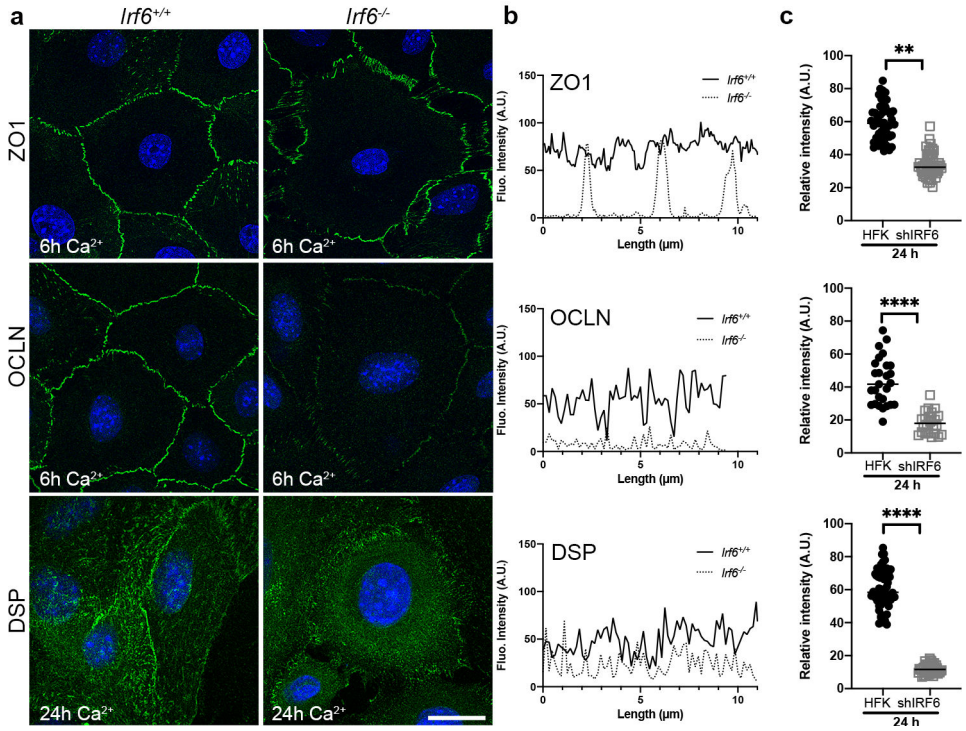

Figure 2: IRF6 is required for tight junction and desmosomal protein localization at the membrane.

(**a**) Immunofluorescence staining (green) for ZO1, Occludin (OCLN), and Desmoplakin (DSP) on *Irf6*$^{+/+}$ and *Irf6*$^{-/-}$ keratinocytes 6 h or 24 h following high [Ca^{2+}] treatment. Nuclear DNA is labeled with DAPI (blue). Scale bar = 25 μm (**b**) Line scan of fluorescent intensity at the membrane of cells shown in (**a**). (**c**) Quantification of fluorescence intensity at the membrane 6 h and 24 h following high [Ca^{2+}] treatment in HFK and shIRF6 keratinocytes. Because the Desmoplakin signal was too weak after 6 h of calcium treatment, only the 24 h time point is shown. ** $P < .01$, and **** $P < .0001$ following Kruskal-Wallis test with Dunn's multiple comparison post-hoc test. Only relevant significance is presented.

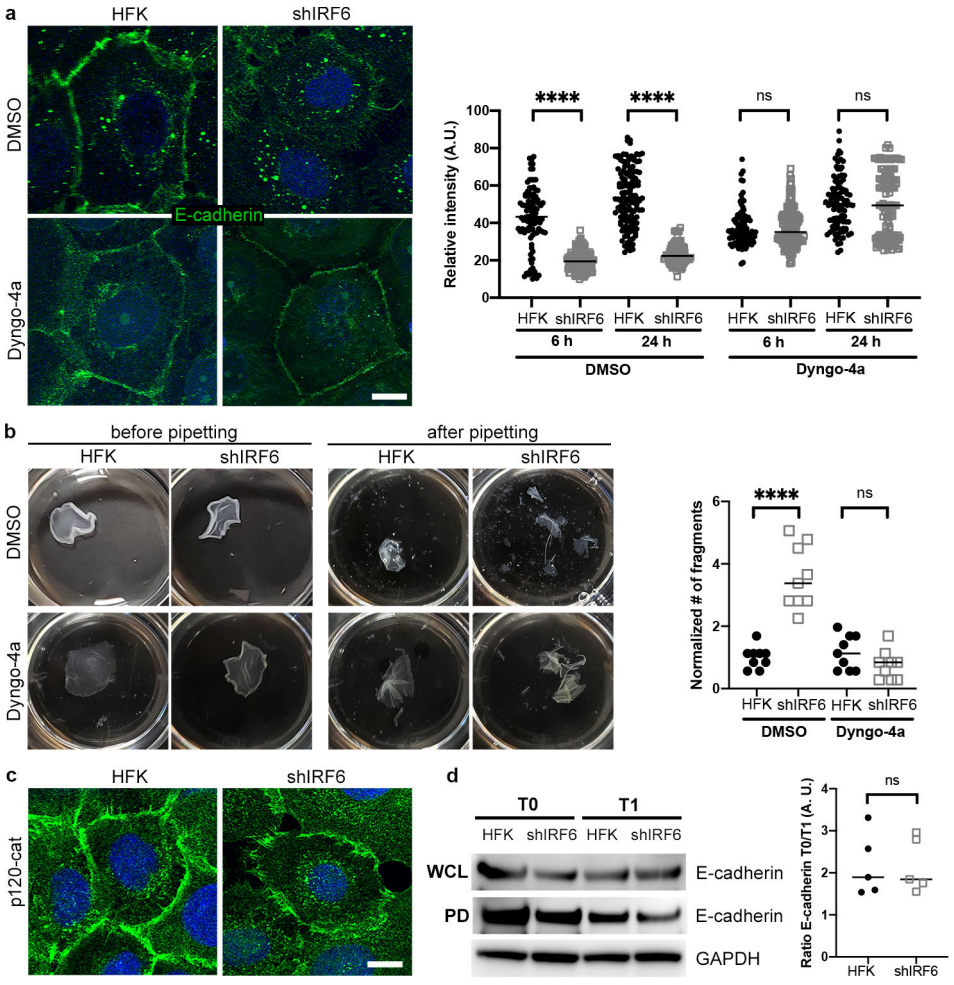

Figure 3: IRF6 is not required for E-cadherin endocytosis.

(**a**) Immunofluorescent staining of HFK and shIRF6 for E-cadherin 24 h in high [Ca^{2+}], in the presence of DMSO or Dyngo-4a. Quantification of fluorescence intensity at the membrane 6 and 24 h following [Ca^{2+}] treatment in HFK and shIRF6 keratinocytes in DMSO and Dyngo-4a. (**b**) Macroscopic images showing HFK and shIRF6 confluent monolayer following Dispase II treatment before and after mechanical disruption in DMSO or treated with Dyngo-4a. Quantification of number of fragments per well normalized to HFK is presented (right panel). (**c**) Immunofluorescent staining of HFK and shIRF6 for p120-catenin 24 h in high [Ca^{2+}]. (**d**) Total cell surface proteins were purified using labelling with biotin (Input) and pulled down via avidin affinity (Pull down). Proteins were extracted immediately (T0) or 1 hour (T1) at 37°C following biotinylation. Immunoblots for E-cadherin in HFK and in shIRF6 keratinocytes. GAPDH was used as loading control. Intensity of E-cadherin signal was quantified and ratio T0/T1 compared between HFK and shIRF6. ns = not significant after Student's *t*-test. For (a) and (b), **** $P < .0001$, ns = not significant after Kruskal-Wallis test with Dunn's multiple comparison post-hoc test. Only relevant significance is presented.

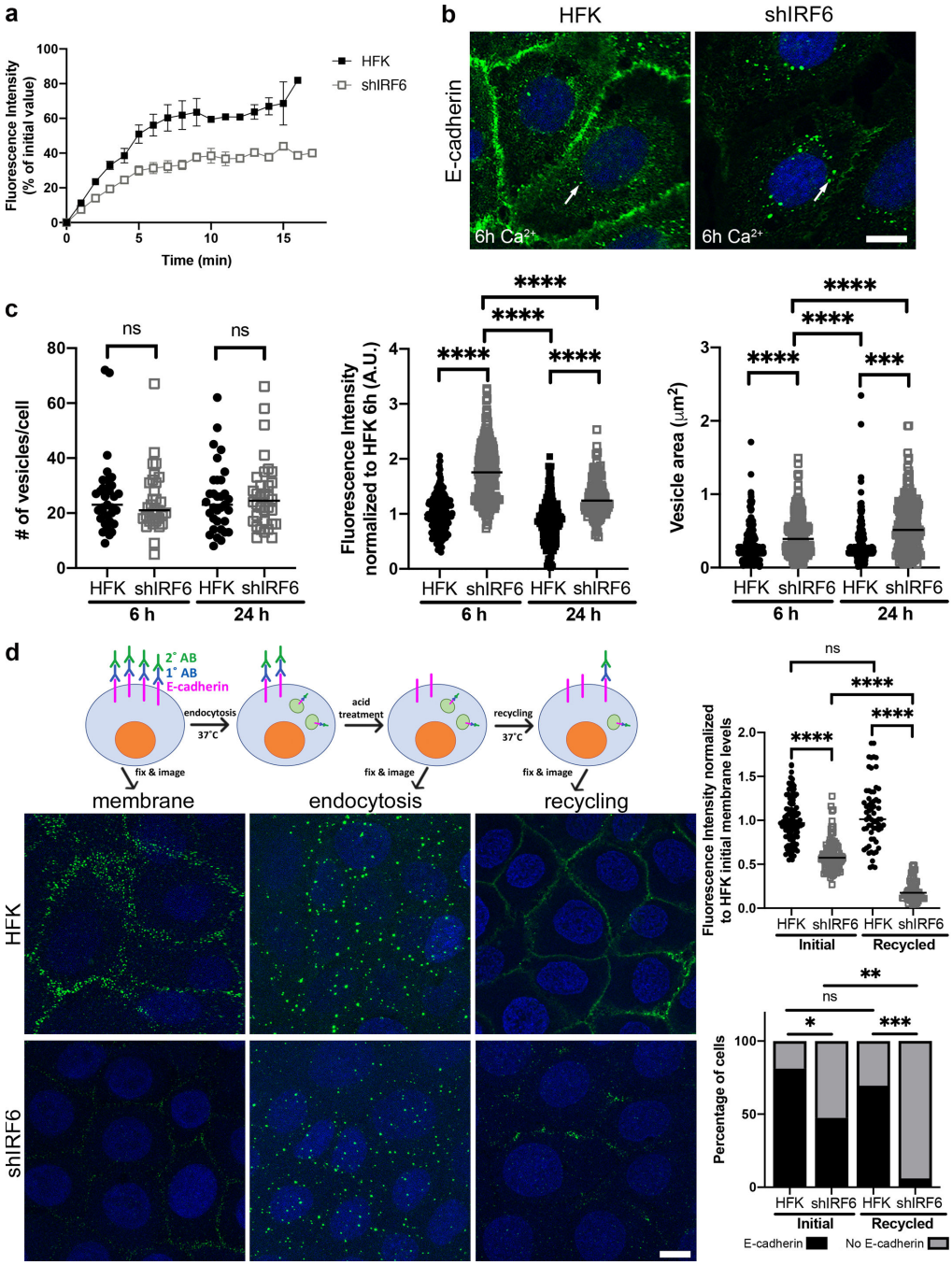

Figure 4: IRF6 impacts E-cadherin trafficking to the plasma membrane.

(**a**) Fluorescence recovery after photobleaching of HFK and shIRF6 transfected with E-cadherin-GFP. (**b**) Immunofluorescent staining of HFK and shIRF6 for E-cadherin 6 h following high [Ca^{2+}] treatment. White arrows indicate E-cadherin positive cytoplasmic vesicles. (**c**) Quantification of number, intensity of fluorescence, and area of vesicles in HFK and shIRF6. A minimum of 50 cells were counted per group in three separate experiments. (**d**) Internalization of E-cadherin in HFK or shIRF6 cells 60 min after addition of E-cadherin antibody. Representative images of E-cadherin antibody at the membrane, endocytosed,

and recycled. Scale bars = 10 μm. Graph on the top right represents the quantification of E-cadherin fluorescence intensity (normalized) at the membrane at the beginning of the internalization assay (“Initial”) and following recycling at the membrane (“Recycled”) in HFK and shIRF6 keratinocytes. **** $P < .0001$ following Mann-Whitney test. Graph on the bottom right represent the percentage of cells with or without E-cadherin at the membrane at the beginning of the assay and following recycling at the membrane.